STRONG 2020 Fixed target experiments at LHC

Heavy flavor production in heavy-ion collisions

Bojana Ilic,

Institute of Physics Belgrade

European Research Council
Established by the European Commission

МИНИСТАРСТВО ПРОСВЕТЕ, НАУКЕ И ТЕХНОЛОШКОГ РАЗВОЈА

In collaboration with: Magdalena Djordjevic (P.I.), Dusan Zigic, Stefan Stojku, Jussi Auvinen, Igor Salom, Marko Djordjevic and Pasi Huovinen

Our goals

I. Introducing the DREENA framework and testing its ability to additionally constrain bulk QGP properties through high-p_T sector

Constant T medium:

II. Utilizing complex R_{AA} patterns to differentiate between major energy loss mechanisms

III. Focusing on the region p_T<50 GeV and addressing:

- Which observable could isolate collisional from radiative energy loss
- Analytical derivation of an explicit relation between collisional suppression/energy loss and heavy quark mass
- Analytical and numerical derivation of the mass hierarchy in collisional energy loss through this observable

D. Zigic, I. Salom, J. Auvinen, P. Huovinen and M. Djordjevic, arXiv:2110.01544
M. Djordjevic, PLB 763, 439
B. Ilic and M. Djordjevic, arXiv:2203.06646 [hep-ph], PRC in press

I. Introducing DREENA framework and testing its ability to further constrain bulk QGP properties

The dynamical energy loss formalism

Features:

- QCD medium of finite size and finite temperature
- The medium consists of dynamical (i.e., moving) partons
- Based on finite T field theory and generalized HTL approach M. Djordjevic, PRC 74, 064907; PRC 80, 064909, M. Djordjevic, U. Heinz, PRL 101, 022302
- The same theoretical framework for both radiative and collisional energy loss
- Applicable to both light and heavy flavor M. Djordjevic and M. Gyulassy, Nucl. Phys. A 733, 265
- Finite magnetic mass effects M. Djordjevic and M. Djordjevic, PLB 709, 229
- Running coupling M. Djordjevic and M. Djordjevic, PLB 734, 286
- Relaxed soft-gluon approximation B. Blagojevic, M. Djordjevic, M. Djordjevic, PRC 99, 024901

✓All these ingredients important for adequately addressing the data B. Blagojevic and M.Djordjevic, JPG 42, 075105
✓No fitting parameters
✓Temperature as a natural variable in the model

Experimental validation of dynamical energy loss formalism

PLB 734, 286

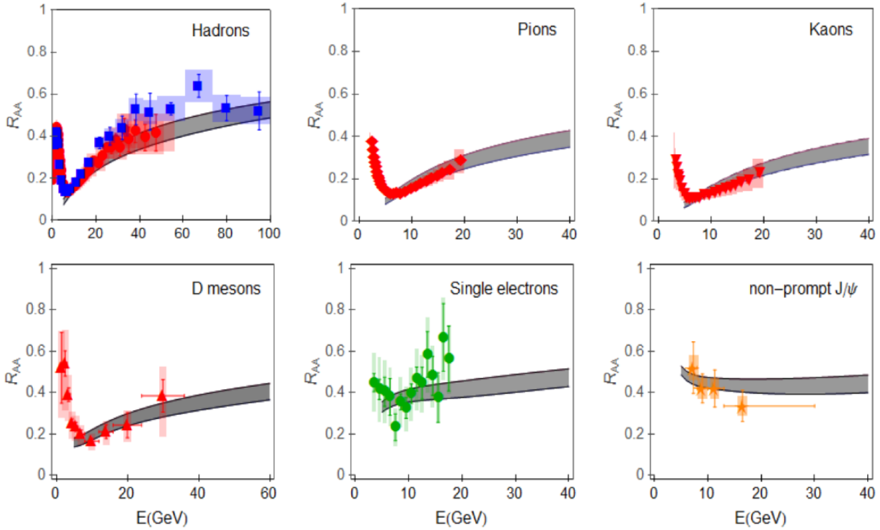

PRC 94, 044908

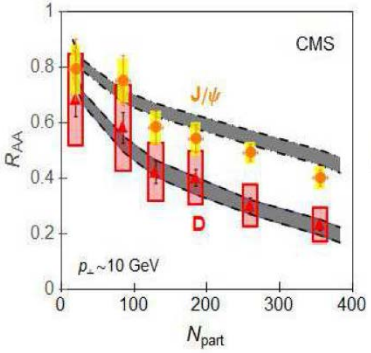

PLB 763, 439

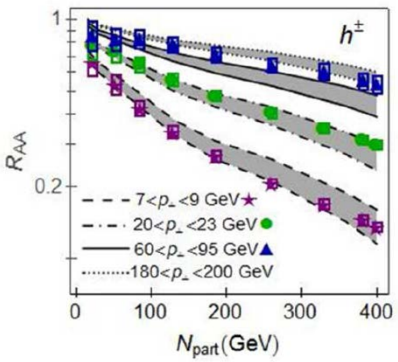

Explains high-p⊥ R_{AA} data for different probes, collision systems (experiments), energies and centralities!

PRC 90, 034910

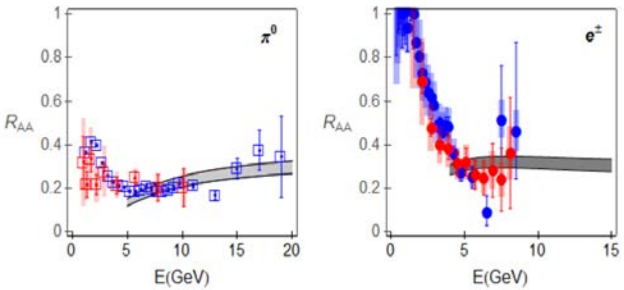

PRL 112, 042302

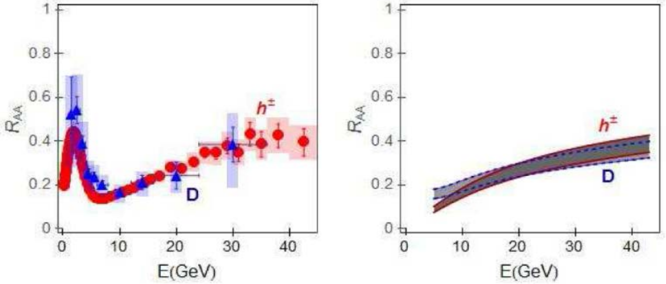

Addresses heavy-flavor puzzle.

PRC 92, 024918

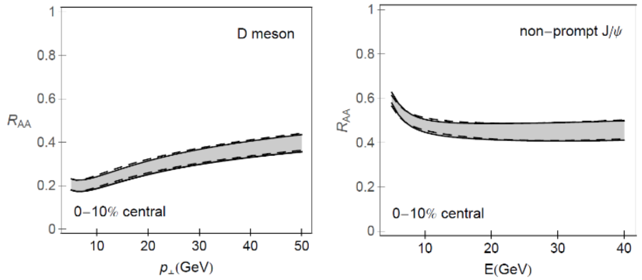

2.76 TeV vs 5.02 TeV

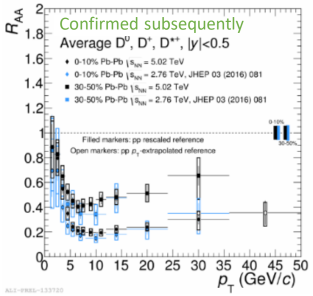

Clear predictive power.

Accurately addresses parton-medium interactions → Suitable for these studies!

DREENA-A framework as a QGP tomography tool

For using high-p_T theory/data to study the bulk QGP properties:

- Include arbitrary medium evolution (T profile) as the only input (both averaged and ebe)
- Preserve all dynamical energy loss model ingredients
- Develop an efficient (timewise) numerical procedure
- Produce a wide set of light and heavy flavor suppression predictions
- Compare predictions with the data
- (Iterate comparison for different combinations of QGP parameters)
- Constrain medium properties consistent with both low- and high-p_T sector

⇩

Fully optimized DREENA-A (Dynamical Radiative and Elastic ENergy loss Approach, A – Adaptive temperature profile) framework.

D. Zigic, I. Salom, J. Auvinen, P. Huovinen and M. Djordjevic, arXiv:2110.01544

Could high-p_T theory/data provide a constraint on different medium evolution models?

τ_0=1 fm

τ_0=0.2 fm

τ_0=1.16 fm

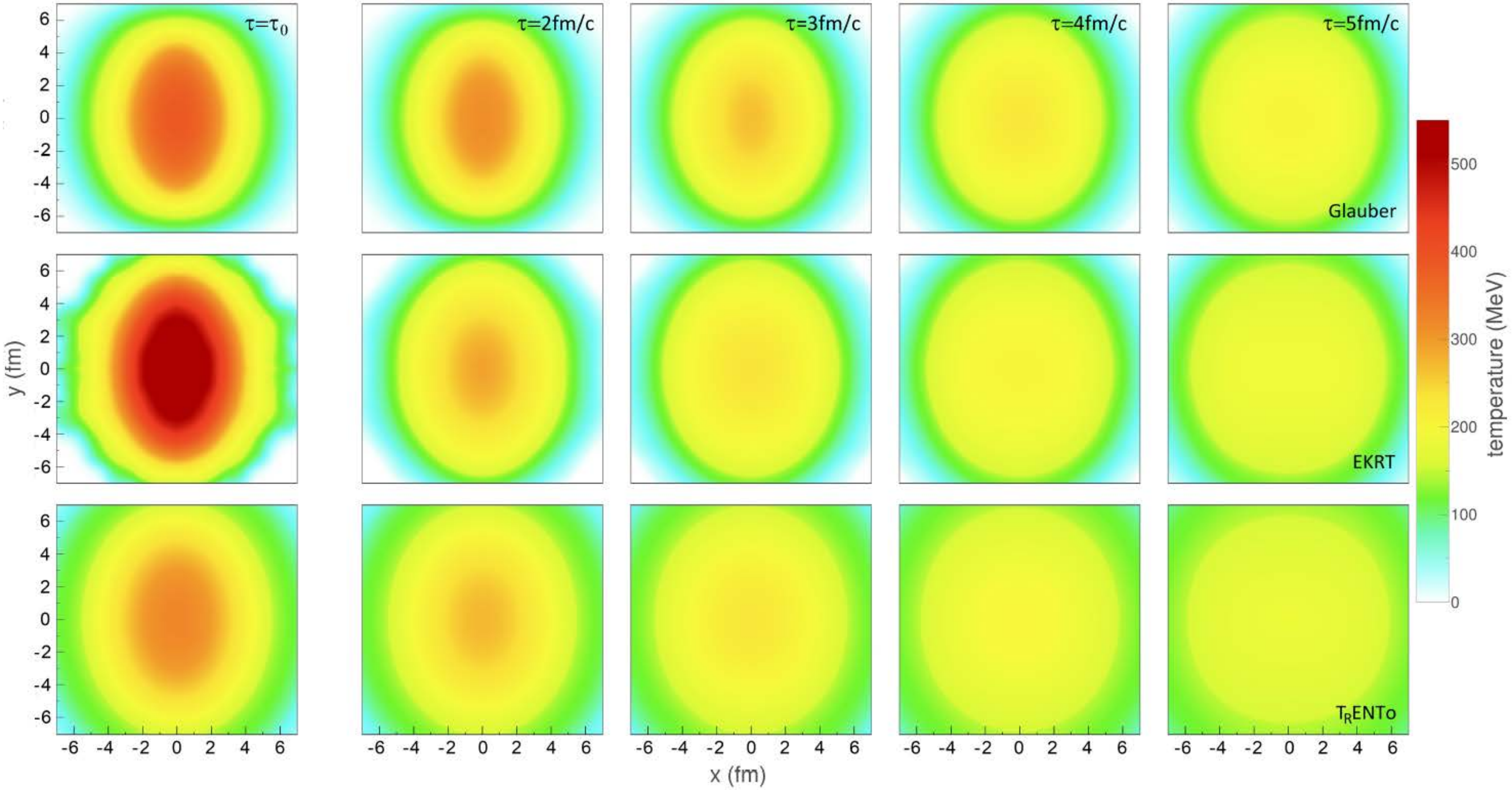

All three evolutions agree with low- p_T data.

Could high-p_T sector additionally constrain these evolutions?

D. Zigic, I. Salom, J. Auvinen, P. Huovinen and M. Djordjevic, arXiv:2110.01544

Qualitative observations

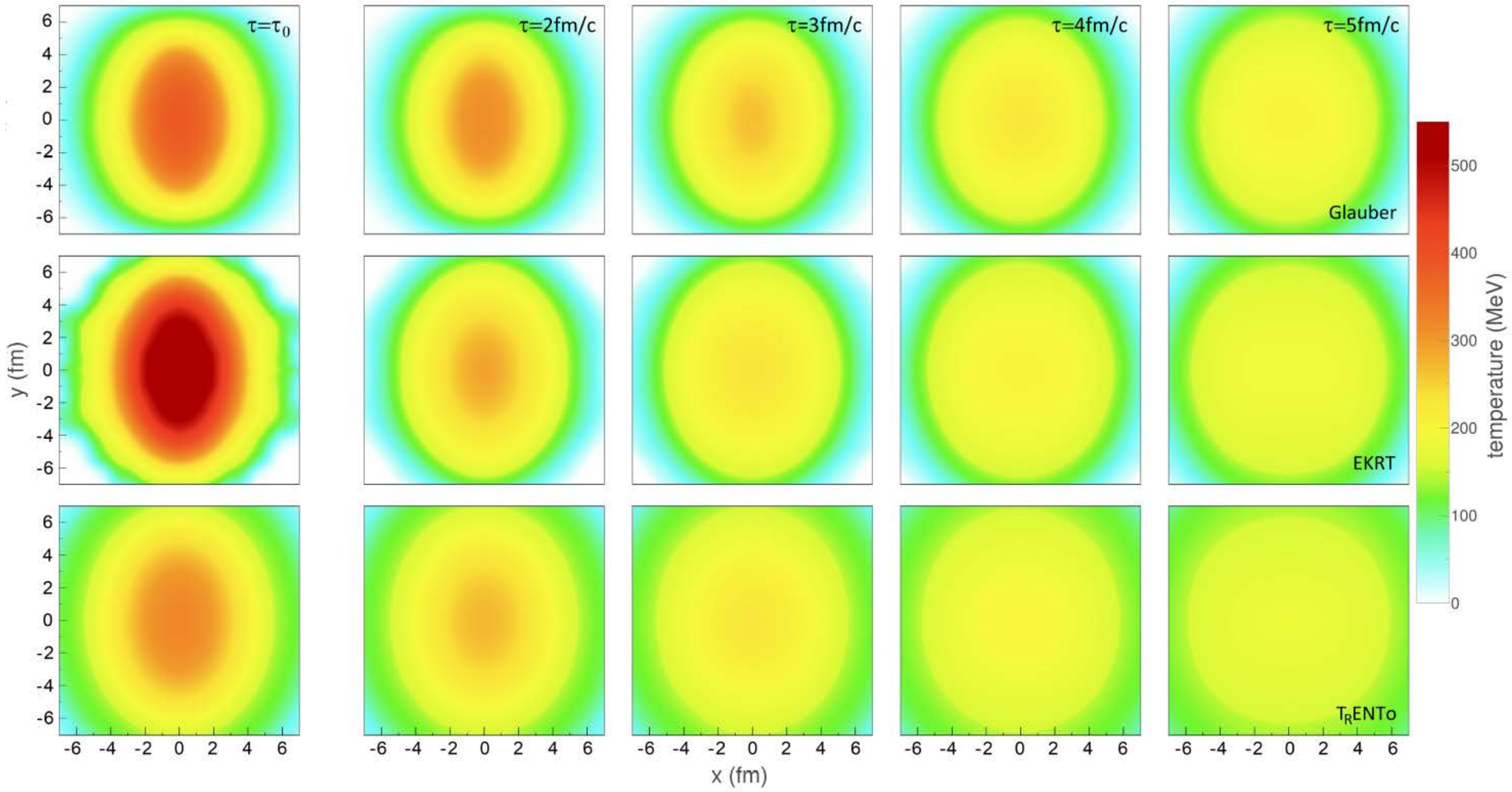

'EKRT' shows the largest T → expected the smallest R_{AA}

Asymmetry: 'Glauber'>'EKRT' >'T_RENTo' → expected v_2(Glauber)> v_2(EKRT)> v_2(T_RENTo)

D. Zigic, I. Salom, J. Auvinen, P. Huovinen and M. Djordjevic, arXiv:2110.01544

Test of DREENA-A predictions

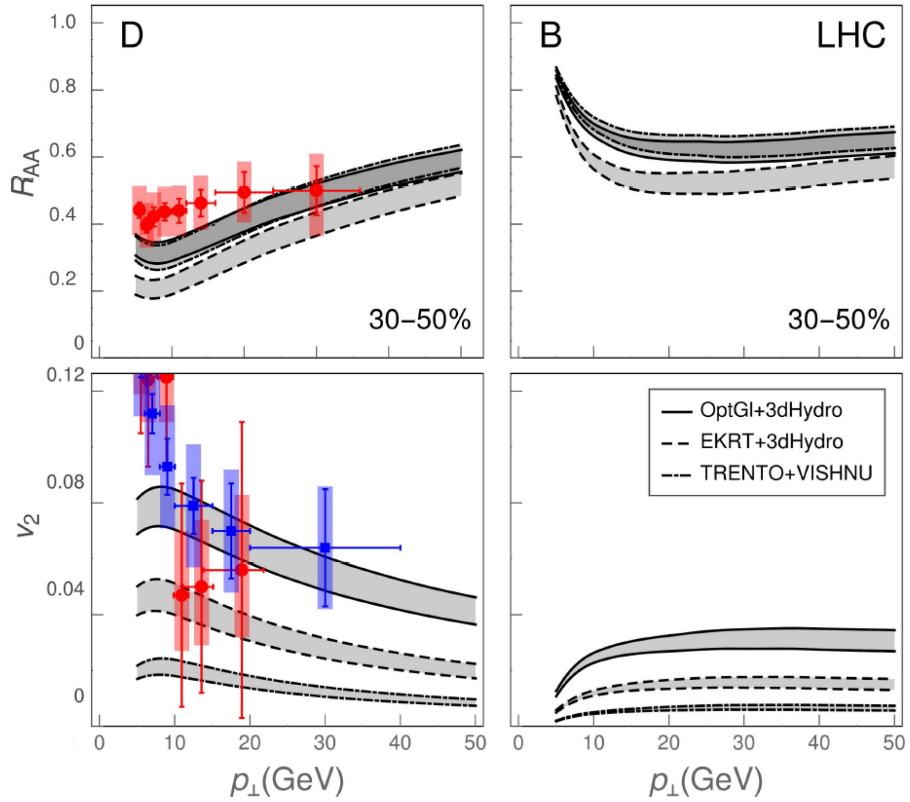

ALICE: JHEP 10, 174; PRL 120, 102301
CMS: PRL 120, 202301

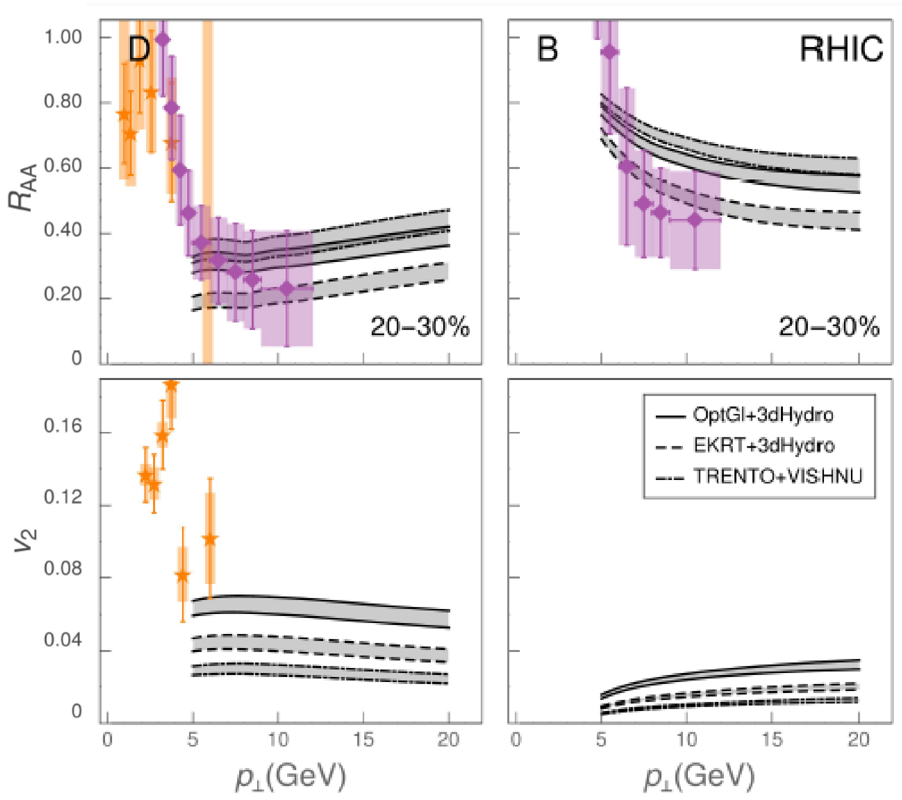

STAR: PRL 121, 229901; PRL 118, 212301

Agreement with RHIC and LHC.

Expect akin conclusions in fixed-target experiments.

'EKRT' results in the smallest R_{AA}

The same v_2 ordering as the system anisotropy ('Glauber' the largest v_2, '$\mathrm{T_RENTo}$' the lowest v_2)

Different T profiles: DREENA-A can distinguish between them → complement constraint to low-p_T sector.

D. Zigic, I. Salom, J. Auvinen, P. Huovinen and M. Djordjevic, arXiv:2110.01544

The role of higher harmonics in QGP tomography

ebe

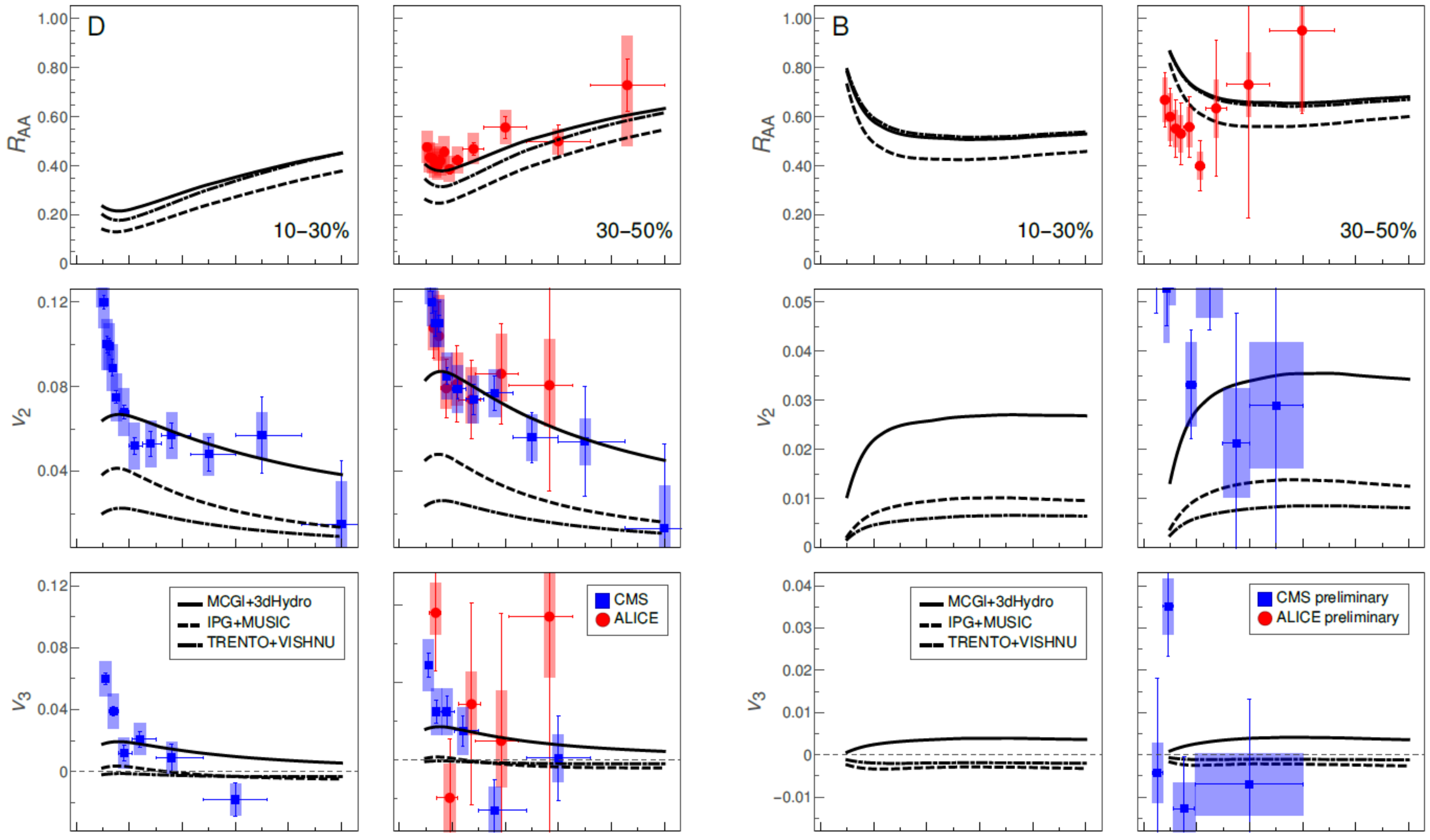

ALICE: JHEP 01, 174; PLB 813, 136054. CMS: PLB 816, 136253

ALICE: arXiv: 2202.00815. CMS: Y. Kim, QM22

Later thermalization time favored and v_2 ordering as for averaged profiles.

Higher harmonics: qualitatively and quantitatively differentiate between medium evolutions!

More sensitive!

Good observables for imposing additional constraints on bulk QGP parameters!

MC-Glauber τ_0=1 fm
IP_Glasma τ_{switch}=0.4 fm
T_RENTo τ_0=1.16 fm

Heavy-flavor high- p_T observables more sensitive than light flavor!

D. Zigic, J. Auvinen, I. Salom, P. Huovinen and M. Djordjevic, in preparation

II. Utilizing complex R_{AA} patterns to differentiate between major energy loss mechanisms (T=const)

Numerical framework: DREENA-C

D. Zigic, I. Salom, J. Auvinen, M. Djordjevic and M. Djordjevic, J. Phys. G 46, no.8, 085101

- Full-fledged DREENA-C (Dynamical Radiative and Elastic ENergy loss Approach, C stands for constant/average temperature profile) framework:
  - Dynamical energy loss formalism:
    - ✓Complex, unique and realistic features
    - ✓Dominant ingredient for generating high-$p_\perp$ suppression predictions
  - Constant (average) Temperature profile:
    - ✓Excludes complications from details of medium evolution
    - ✓Analytical derivations feasible
    - ✓Insignificant loss of accuracy in R_{AA} predictions (compared to DREENA-B (PLB 791, 236) and DREENA-A), low R_{AA} sensitivity to details of medium evolution

JPG 46, 085101; PLB 791, 236; PRC 99, 061902(R); PRC 85, 044903; NPA 932, 140

DREENA-C is an optimal framework for these studies (II and III), through R_{AA}, as it assumes sophisticated energy loss model.

JPG 42, 075105

Nonintuitive suppression patterns (light or D probes)

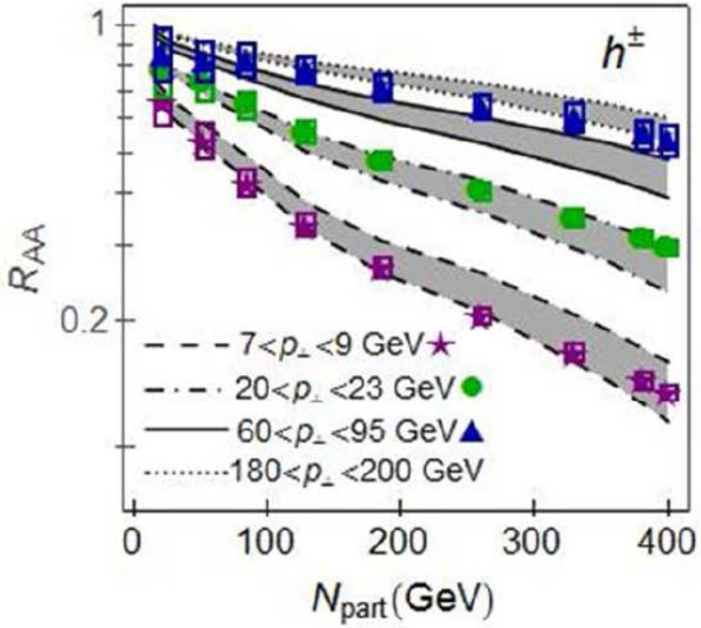

With increasing p_T, R_{AA} vs. N_{part} :

- flatter
- difference between curves smaller

Saturation in R_{AA} vs. N_{part}.

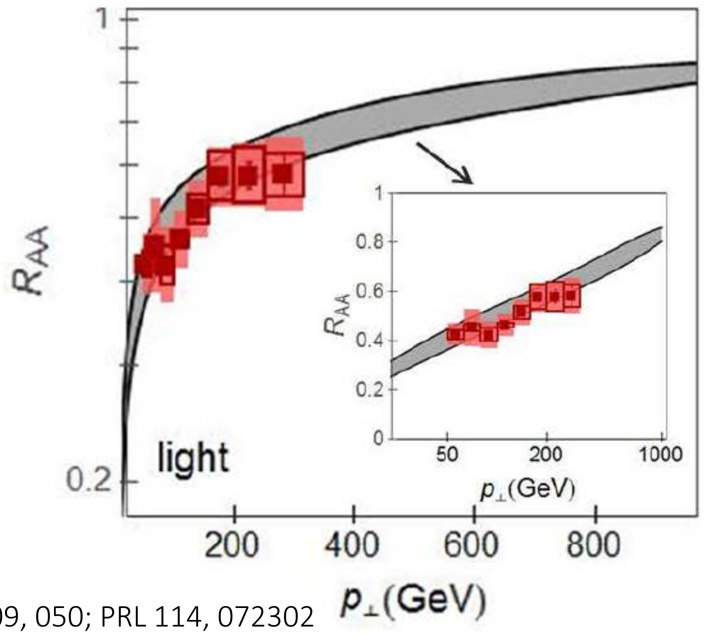

With increasing p_T, R_{AA} vs. p_T flatter.

Saturation in R_{AA} vs. p_T.

Nonintuitive observations in agreement with our framework!

Which energy loss mechanism is accountable for these observations?

M. Djordjevic, PLB 763, 439

ATLAS: JHEP 09, 050; PRL 114, 072302

Nonintuitive suppression patterns (B probes)

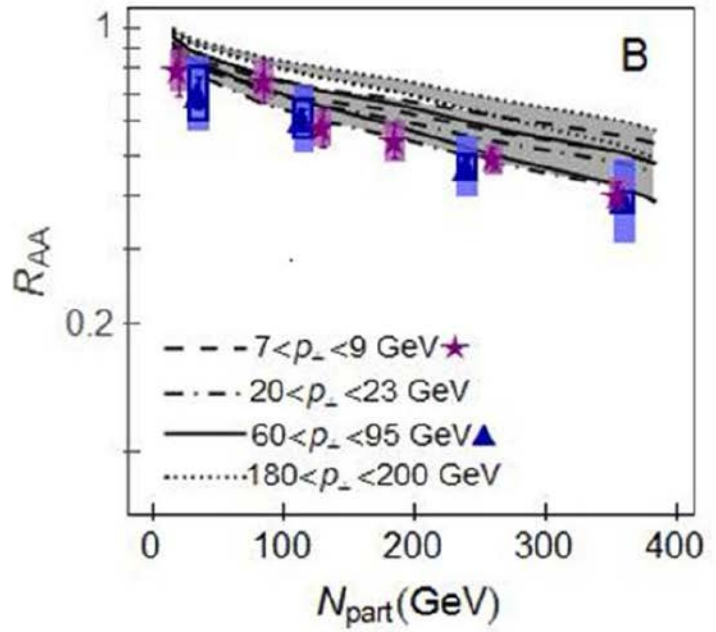

R_{AA} vs. N_{part} pattern qualitatively different (compared to light probes)

Flatter R_{AA} vs. N_{part} across the p_T range

Nonintuitive observation well reproduced within our framework!

Which energy loss mechanism is accountable for these observations?

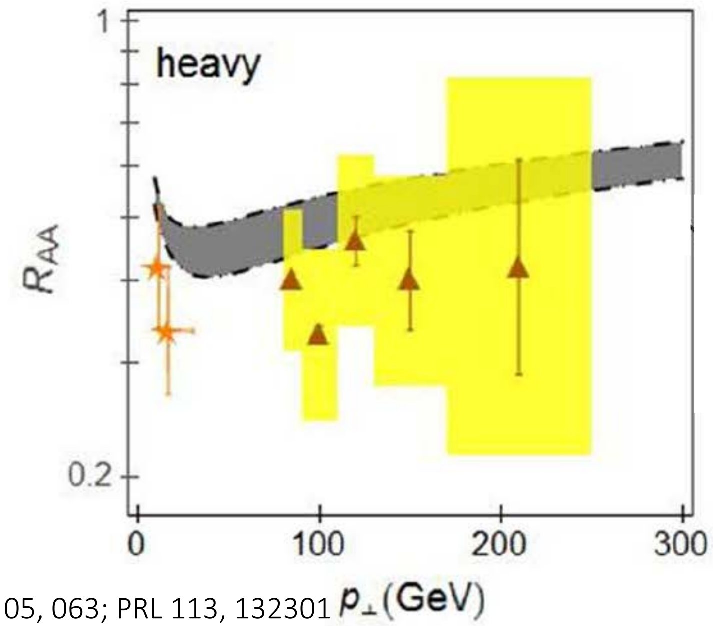

Slower R_{AA} vs. p_T change (compared to light probes)

CMS: JHEP 05, 063; PRL 113, 132301

M. Djordjevic, PLB 763, 439

Qualitative explanation of the observations (light or D probes)

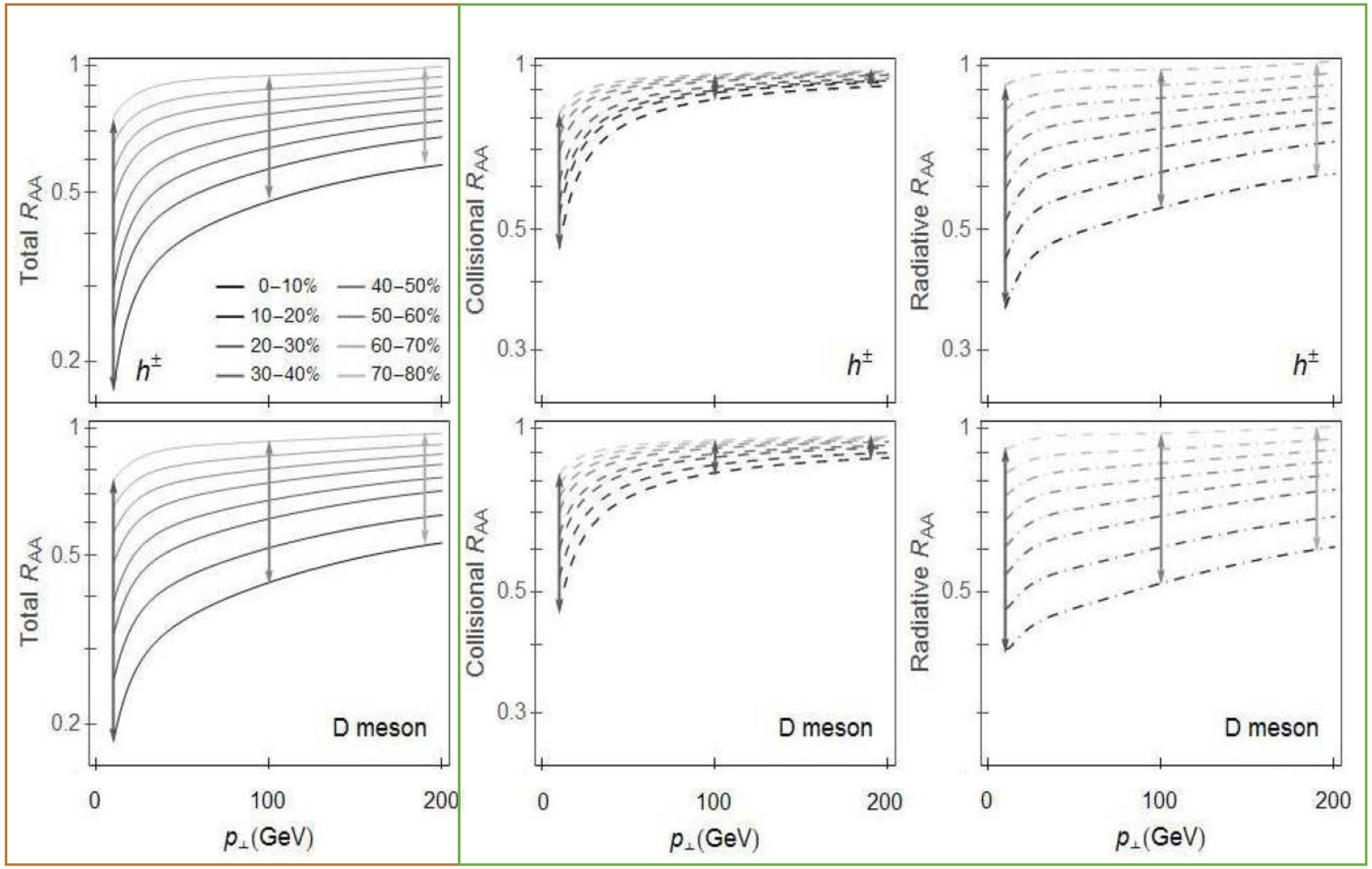

M. Djordjevic, PLB 763, 439

Collisional contribution: significant at <u>lower p_T</u> (steep increase)

Radiative contribution: important at <u>entire p_T</u> range (slow increase)

R_{AA} *vs.* p_T pattern result of interplay of collisional and radiative contributions.

The lower p_T arrow spans a much larger R_{AA} range compared to the larger p_T arrows that are similar.

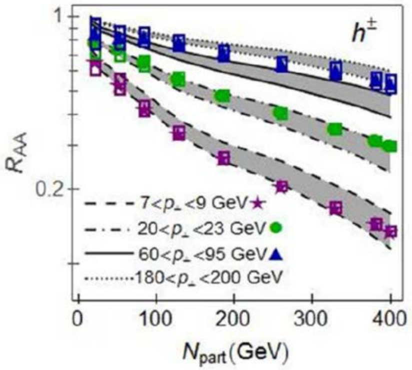

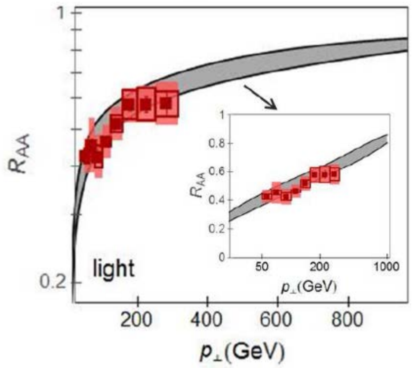

Qualitative explanation of the observations (B probes)

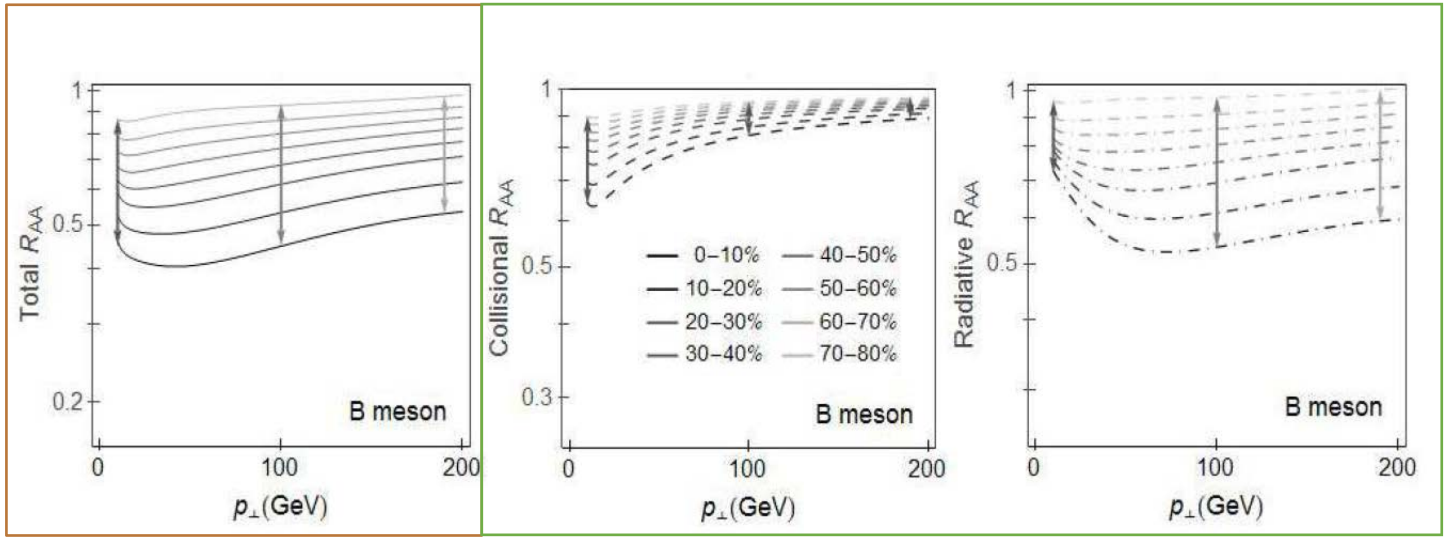

<u>At lower p_T:</u>

Both collisional and radiative contributions significant
(notably smaller than for light/D probes)

R_{AA} vs. p_T pattern consequence of mass hierarchy in collisional and radiative energy losses

<u>At higher p_T:</u>

Nearly flat radiative R_{AA} vs. p_T only important.

R_{AA} vs. p_T curves practically equidistant across the <u>p_T range</u>.

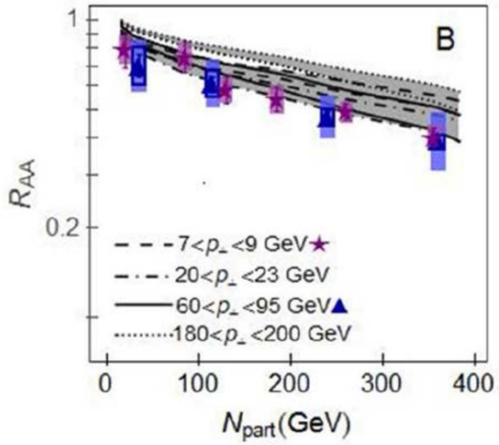

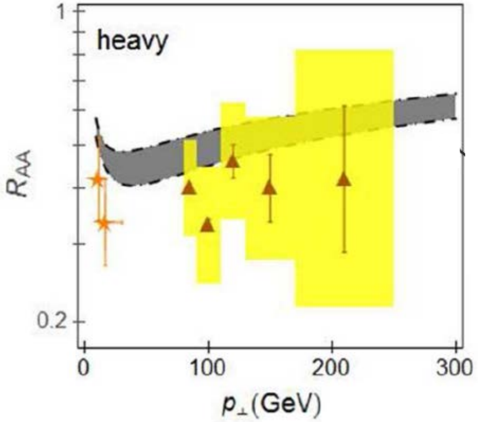

M. Djordjevic, PLB 763, 439

III. Focusing on the region p_T<50 GeV, we present (T=const) :

M. Djordjevic, B. Blagojevic and L. Zivkovic, PRC 94, 044908

A search for an observable, which can unravel collisional from radiative energy loss

Analytical derivation of an exact relation between collisional suppression/energy loss and heavy quark mass for the first time

Analytical and numerical extraction of the mass hierarchy in collisional energy loss through this observable

B. Ilic and M. Djordjevic, arXiv:2203.06646 [hep-ph], PRC in press

Mass hierarchy effect in energy loss mechanisms

- The experimental observations of R_{AA} mass hierarchy (i.e., dead cone) analyzed within radiative models

PLB 519,199; PRD 85, 054012;
PRD 69, 114003; NPA 733, 265; PRC 77, 024905; PLB 763, 439;
PRL 93, 072301

- At intermediate-$p_\perp$ range ($p_\perp \lesssim 10$ GeV) charm and bottom collisional – comparable to (or even larger) than radiative energy loss

NPA 784, 426; PRC 74, 064907; JPG 42, 075105; PLB 273, 128; PRC 72, 014905; APHA 22, 93

- The mass hierarchy in collisional energy loss is not yet addressed
- The upcoming RHIC and LHC measurements – employ high-p_T heavy flavor data for studying interaction mechanisms in QGP

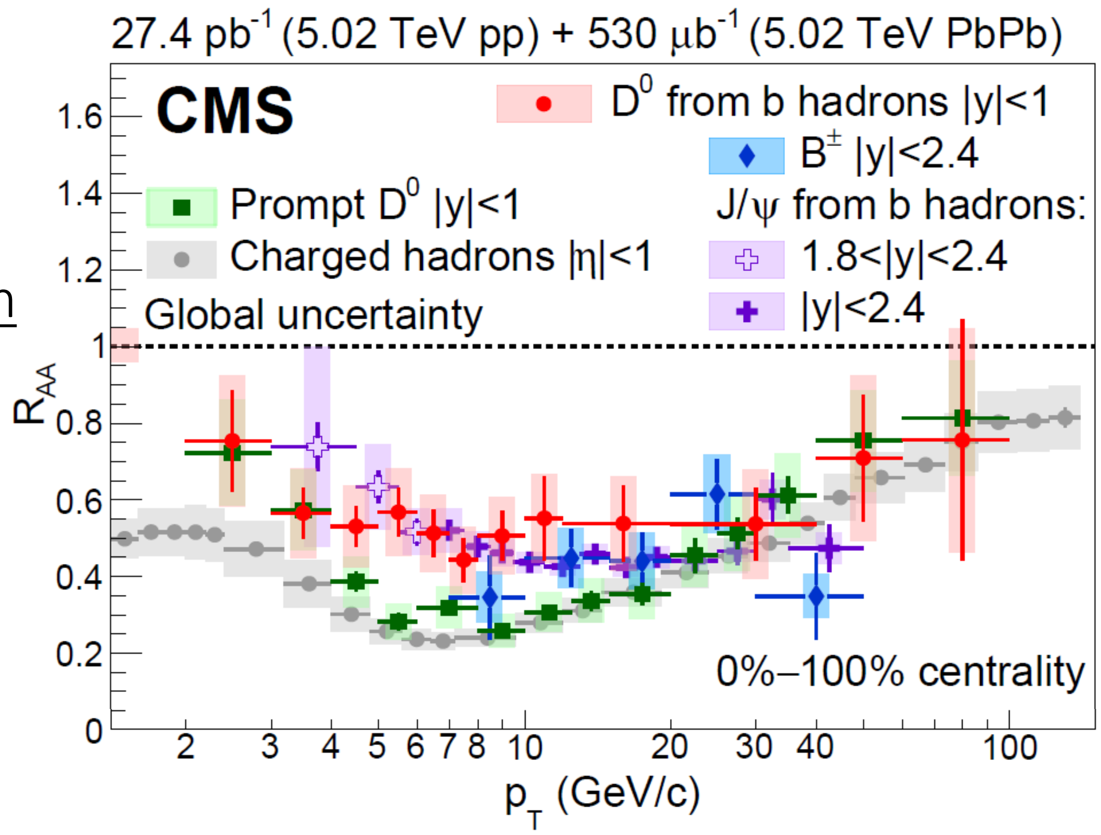

PRL 123 (2019) 022001

B. Ilic and M. Djordjevic, arXiv:2203.06646 [hep-ph], PRC in press

Mass hierarchy in energy loss mechanisms

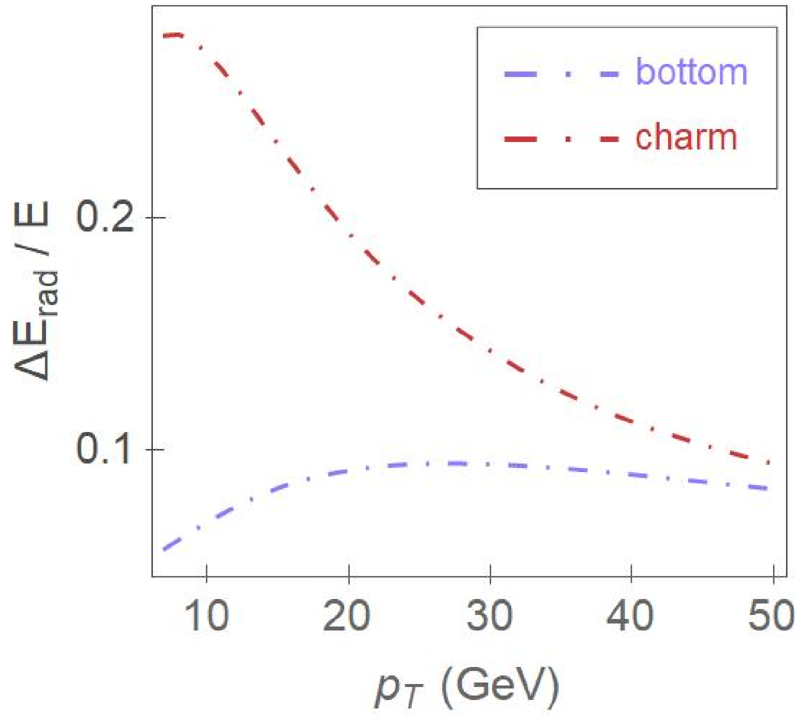

M. Djordjevic, B. Blagojevic and L. Zivkovic, PRC 94, 044908

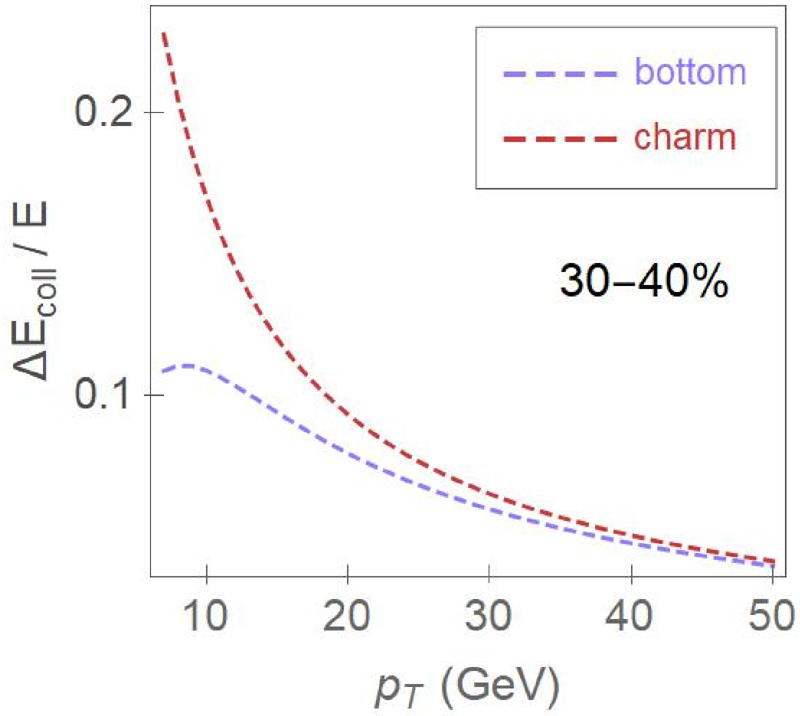

PRC 74, 064907; PRC 93, 014901; NPA 931, 581; arXiv:0812.0270

Which observable could quantify this effect?

Proposition: $f(1 - R_{AA})$, as being particularly sensitive to parton energy loss solely.

PRC 99, 061902(R); PRC 103, 024908

The dead-cone effect, i.e., the mass hierarchy in radiative energy loss.

Importantly: Obtained clear mass hierarchy in collisional energy loss also!

B. Ilic and M. Djordjevic, arXiv:2203.06646 [hep-ph], PRC in press

Search for an observable

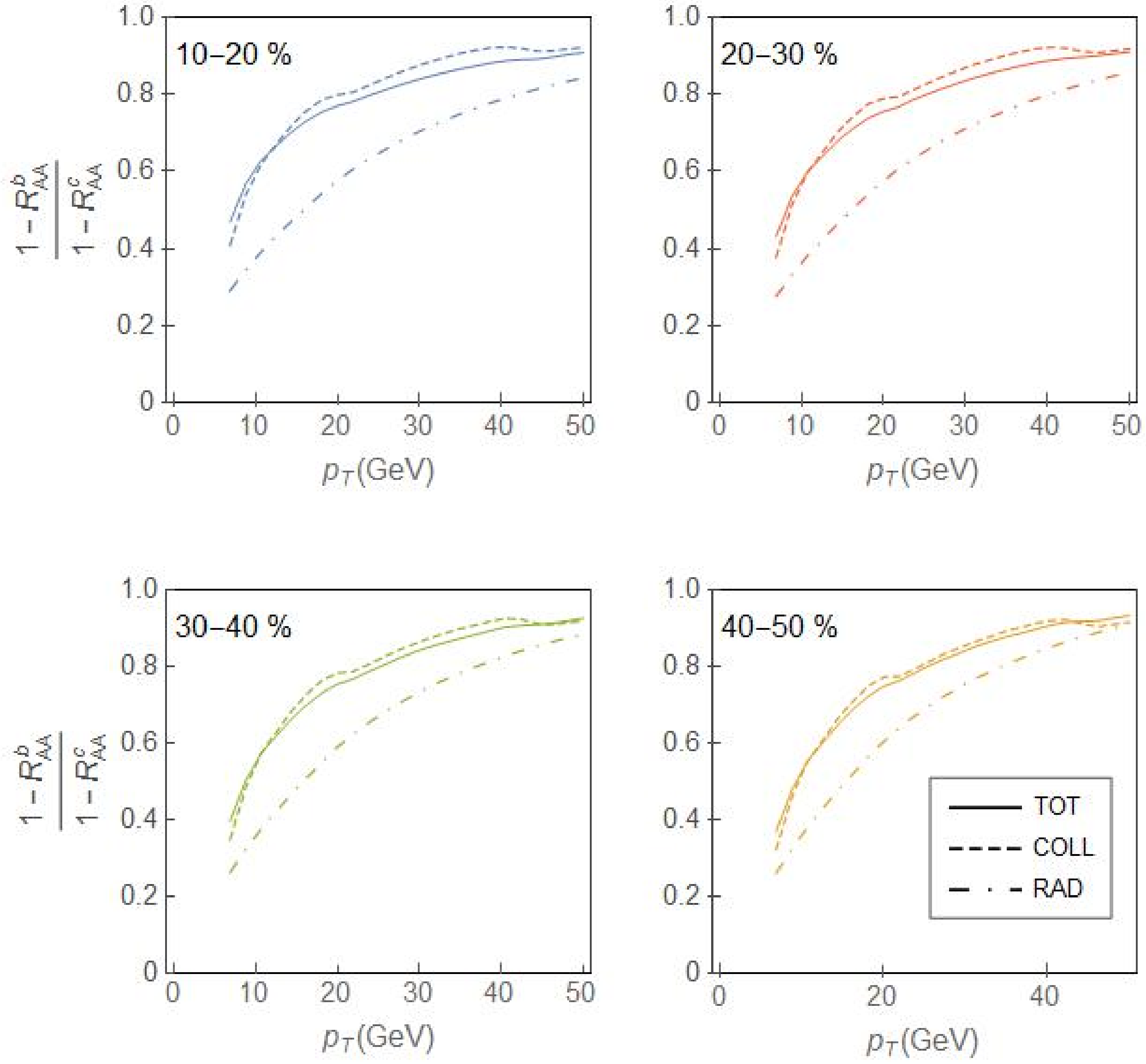

<u>Unexpectedly</u>: For all centralities TOT and COLL ratios nearly overlapping!

Collisional contribution in the origin of heavy flavor $1 - R_{AA}$

$1 - R_{AA}$ ratio might disclose <u>mass hierarchy</u> in collisional energy loss.

B. Ilic and M. Djordjevic, arXiv:2203.06646 [hep-ph], PRC in press

Analytical derivation: Which information does the new observable carry?

Convolution of initial parton p_T distribution and collisional energy loss:

$$\frac{d\sigma^f}{dp_T^2}=\int d\varepsilon D(\varepsilon)\frac{d\sigma^i(p_T+\varepsilon)}{dp_T^2}=\int d\varepsilon D(\varepsilon)\frac{d\sigma^i(p_T)}{dp_T^2}+\int d\varepsilon D(\varepsilon)\frac{\varepsilon}{1!}\frac{d}{dp_T}\left(\frac{d\sigma^i(p_T)}{dp_T^2}\right)+\ldots$$

$$\simeq\frac{d\sigma^i}{dp_T^2}+\Delta E_{coll}\frac{d}{dp_T}\left(\frac{d\sigma^i}{dp_T^2}\right)$$

JHEP 09, 033; PRC 72, 014905

Initial distribution parameterization:

$$\frac{d\sigma^i}{dp_T^2}=\frac{C}{(p_T^2+M^2)^k}$$

PRC 71, 064904

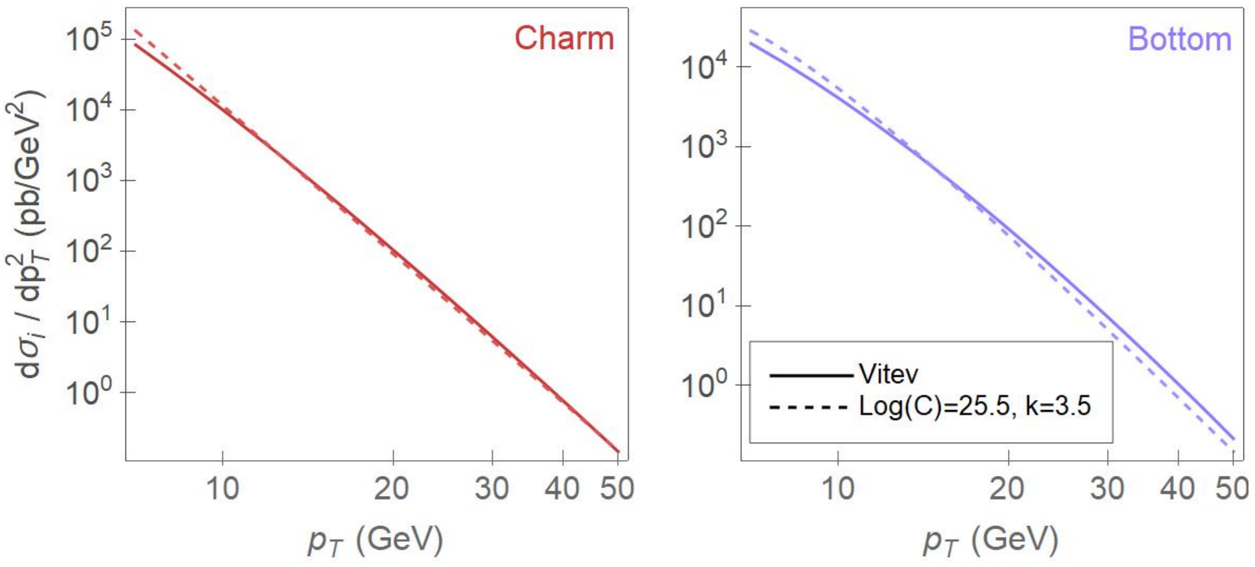

PLB 718, 482; PRC 80, 054902

The same C and k for bottom and charm.

B. Ilic and M. Djordjevic, arXiv:2203.06646 [hep-ph], PRC in press

Analytical derivation: Which information does the new observable carry?

Suppression:

$$R_{AA}=\frac{d\sigma^f}{dp_T^2}\Big/\frac{d\sigma^i}{dp_T^2}$$

PRC 71, 064904

$$1-R_{AA}\simeq 2k\frac{p_T}{E}\frac{\Delta E_{coll}}{E}$$

Collisional energy loss:

$$\frac{\Delta E_{coll}}{E}\sim\frac{1}{Ev^2}\left(v+\frac{v^2-1}{2}\ln\left(\frac{1+v}{1-v}\right)\right)$$

$$v=\frac{p_T}{\sqrt{p_T^2+M^2}}$$

NPB 351 (3), 491

Mass dependence of collisional energy loss:

$$\frac{\Delta E_{coll}}{E}\sim\frac{1}{p_T}\left(1-\frac{M^2}{p_T^2}\ln(2)+\left(\frac{M}{p_T}\right)^{\frac{M}{p_T}+1}-\frac{M}{p_T}\right)$$

Mass dependence of $1-R_{AA}$ ratio:

$$1-R_{AA}\sim\frac{2k}{p_T}\left[1-\frac{M^2}{p_T^2}\left(\ln 2+\frac{1}{2}\right)+\left(\frac{M}{p_T}\right)^{\frac{M}{p_T}+1}-\frac{M}{p_T}\right]$$

Dominant terms

$$\frac{1-R_{AA}^b}{1-R_{AA}^c}\simeq\frac{1-\frac{M_b}{p_T}}{1-\frac{M_c}{p_T}}$$

Carries information about mass hierarchy in collisional energy loss!

New observable

B. Ilic and M. Djordjevic, arXiv:2203.06646 [hep-ph], PRC in press

The new observable $\frac{1-R^b_{AA}}{1-R^c_{AA}}$

Unexpectedly simple relation:

$$\frac{1-R^b_{AA}}{1-R^c_{AA}} \simeq \frac{1-\frac{M_b}{p_T}}{1-\frac{M_c}{p_T}}$$

It is independent of:

- The collision centrality
- The collision system (size)
- The collision energy

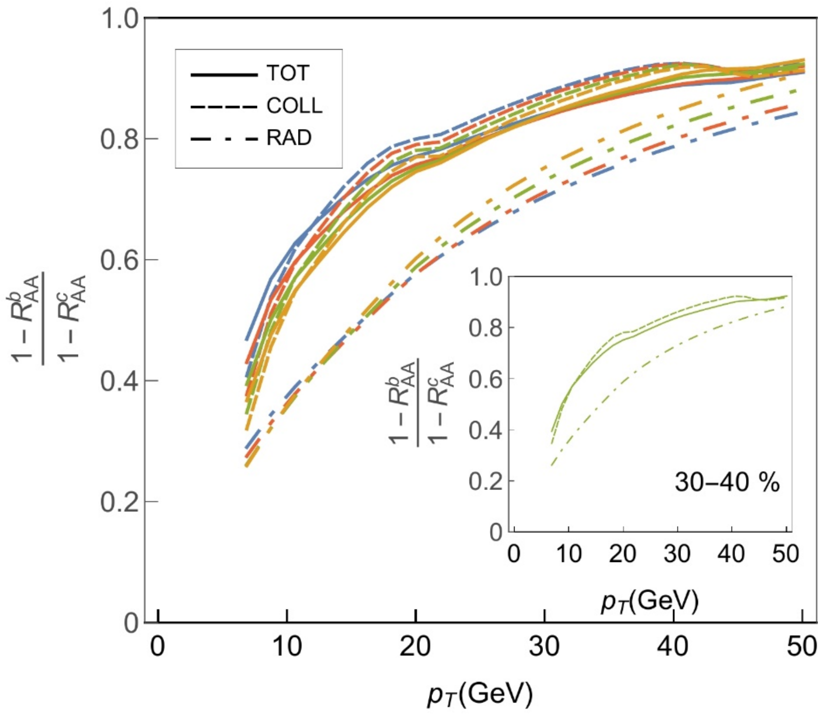

The new observable - applicable to both the RHIC and the LHC experiments.

An open question:

Fixed-target experiments – additional test of our dynamical energy formalism applicability in $\mu_b \neq 0$ regime.

B. Ilic and M. Djordjevic, arXiv:2203.06646 [hep-ph], PRC in press

$$\frac{1-R^b_{AA}}{1-R^c_{AA}} \simeq \frac{1-\frac{M_b}{p_T}}{1-\frac{M_c}{p_T}}$$

Testing the adequacy of new observable $\frac{1-R^b_{AA}}{1-R^c_{AA}}$

A good agreement between:

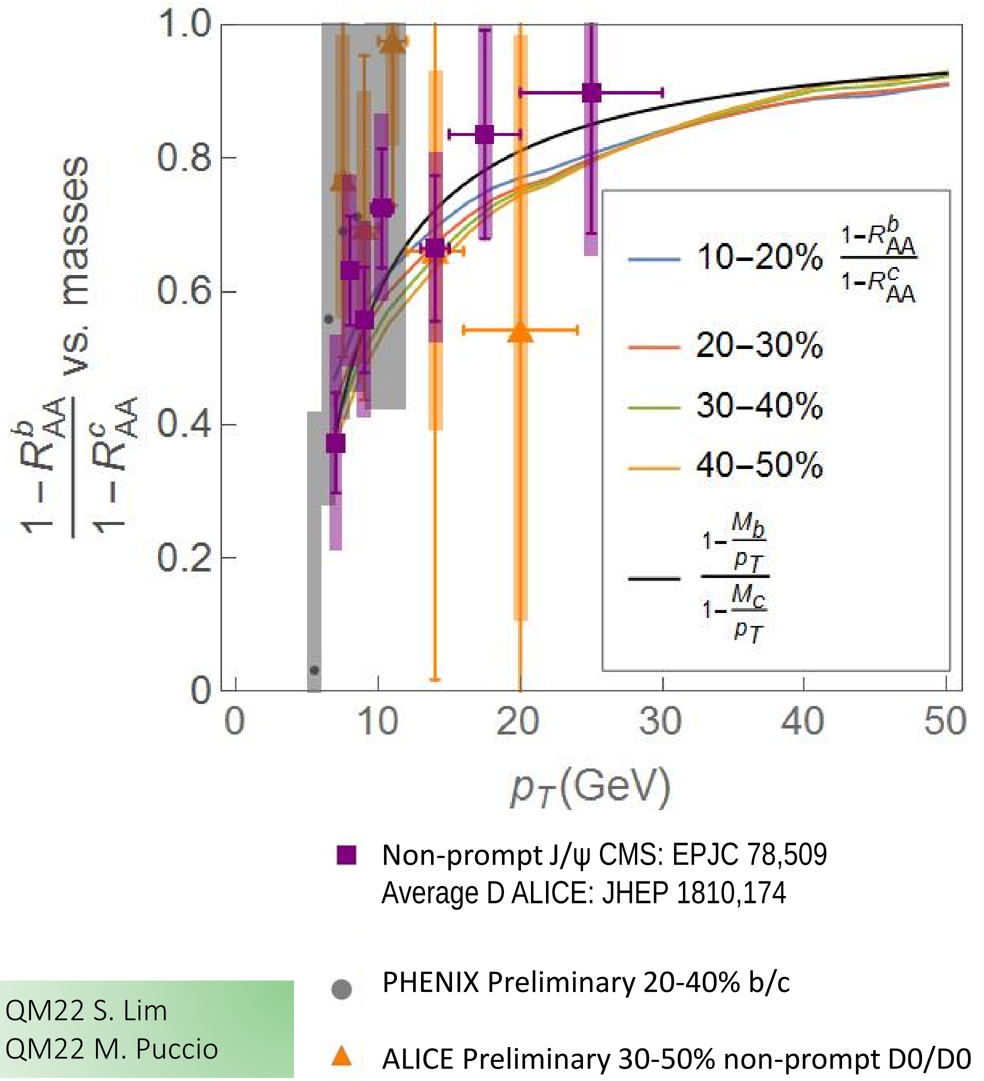

Data and our predictions (qualitatively and quantitatively) ⇒ Confirms adequacy of DREENA-C.

DREENA-C predictions and our analytical estimate $\left(1-\frac{M_b}{p_T}\right)/\left(1-\frac{M_c}{p_T}\right)$ (for all centralities). ⇒ Implies validity of our analysis.

Data and our analytical mass estimate. ⇒ Supports adequacy of proposed observable.

QM22 S. Lim
QM22 M. Puccio

B. Ilic and M. Djordjevic, arXiv:2203.06646 [hep-ph], PRC in press

Conclusions

I. DREENA-A framework – utilizing high-p_T R_{AA} and especially flow harmonics for:
   - Differentiating between diverse medium evolutions
   - Inferring bulk QGP properties

II. Unexpected and significantly different suppression patterns for different flavors - for differentiating between radiative and collisional contributions

III. Focused on p_T <50 GeV region we:
   - Proposed an observable to unravel collisional from radiative energy loss
   - Derived an explicit relation between collisional suppression/energy loss and heavy quark mass
   - Verified the adequacy of the proposed observable against the data
   - Observable robust to collision centrality, system, and energy

Fixed-target experiments - additional test of our dynamical energy loss formalism

Outlook

I. DREENA-A: tomography tool for further constraining bulk properties jointly by low- and high-p_T sector

Future experimental efforts:

II. Single particles measurements at higher p_T
III. Lower p_T, and higher precision measurements→ accessible at both RHIC and LHC
III. B meson (non-prompt J/Ψ, D0) and D meson suppression data should be provided for the same centrality bins

Thank you for your attention!

Backup

Inferring bulk QGP properties through high-p_T sector: ‘Thermalization time’

‘Thermalization time’ τ_0

S. Stojku, J. Auvinen, M. Djordjevic, P. Huovinen and M. Djordjevic, PRC 105, L021901

- The onset of energy loss and transverse expansion
- Important, as early time dynamics is not established yet

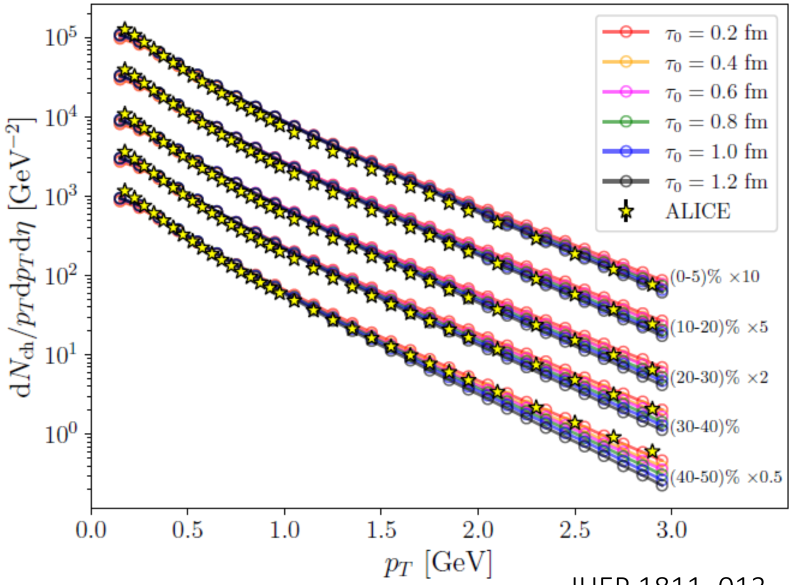

JHEP 1811, 013

E. Molnar, H. Holopainen, P. Huovinen and H. Niemi, PRC 90, 044904

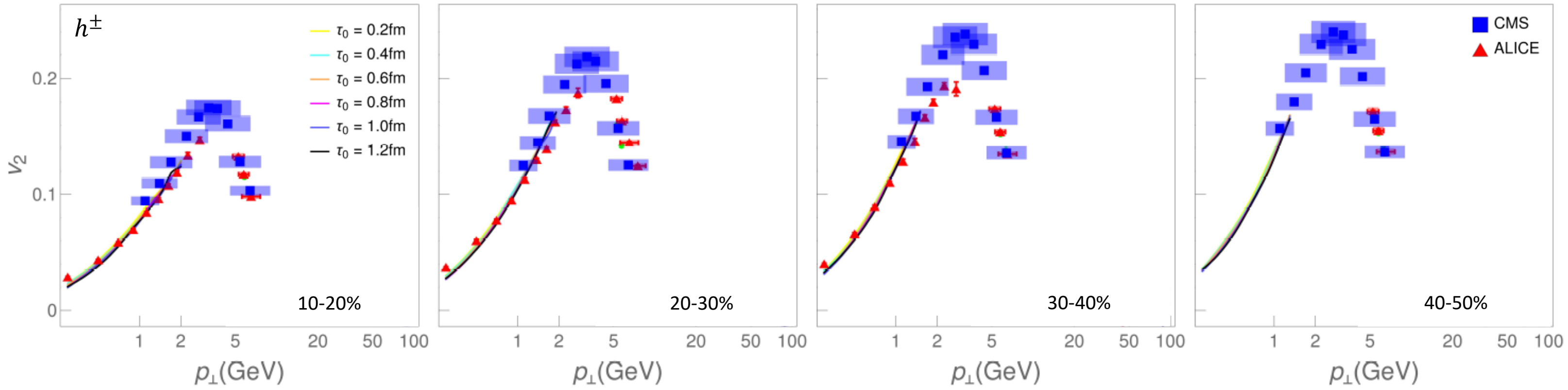

ALICE: JHEP 1807, 103
CMS: PLB 776, 195

Low-p_T sector nearly insensitive to an extensive set of thermalization time (0.2 fm < τ_0 < 1.2 fm); NPA 967, 67

Can high-p_T sector additionally constrain this parameter?

Sensitivity of high- p_T theory and data to thermalization time

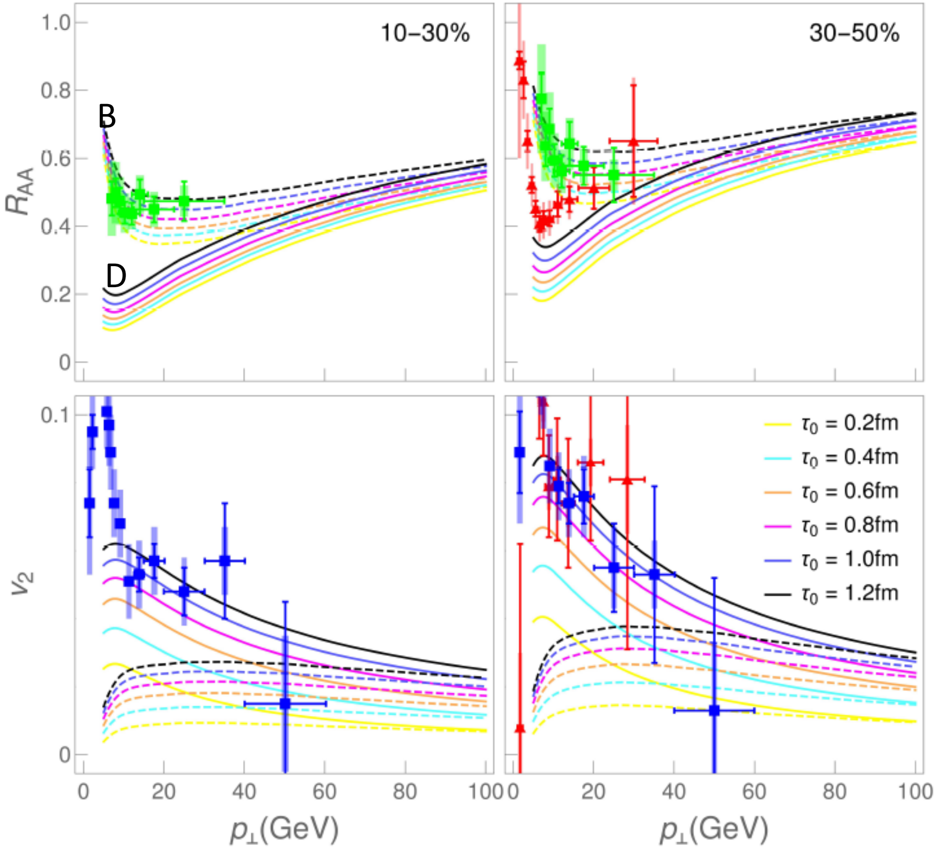

D, ALICE: JHEP 1810, 174; PRL 120, 102301
D, CMS: Phys. Rev. Lett. 120, 202301
B, CMS: EPJC 78, 509

Larger sensitivity of heavy flavors compared to light ones.
(PRC 105, L021901)

High- p_T R_{AA} and v_2 sensitive to τ_0 with preferred later thermalization time!

Larger sensitivity of high-p_T v_2.

QGP tomography: bulk QGP properties jointly constrained by low- and high- p_T sectors.

$v_2 \approx$ difference in R_{AA} (~ T) along in- and out-of-plane directions.

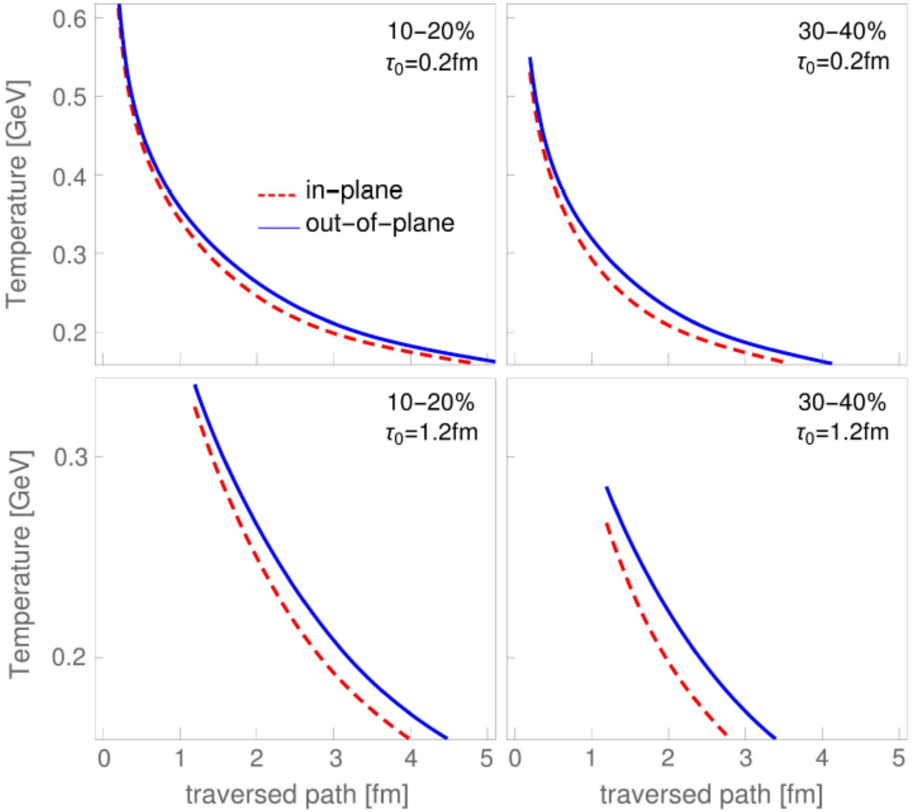

Explanation of v_2 increase with τ_0.

Sensitivity of high-pt theory and data to thermalization time

- Use our DREENA-A framework, which is fully modular, i.e. can include any *T* profile.
- 3+1d hydro profiles with different τ_0 included in DREENA-A to test the sensitivity.

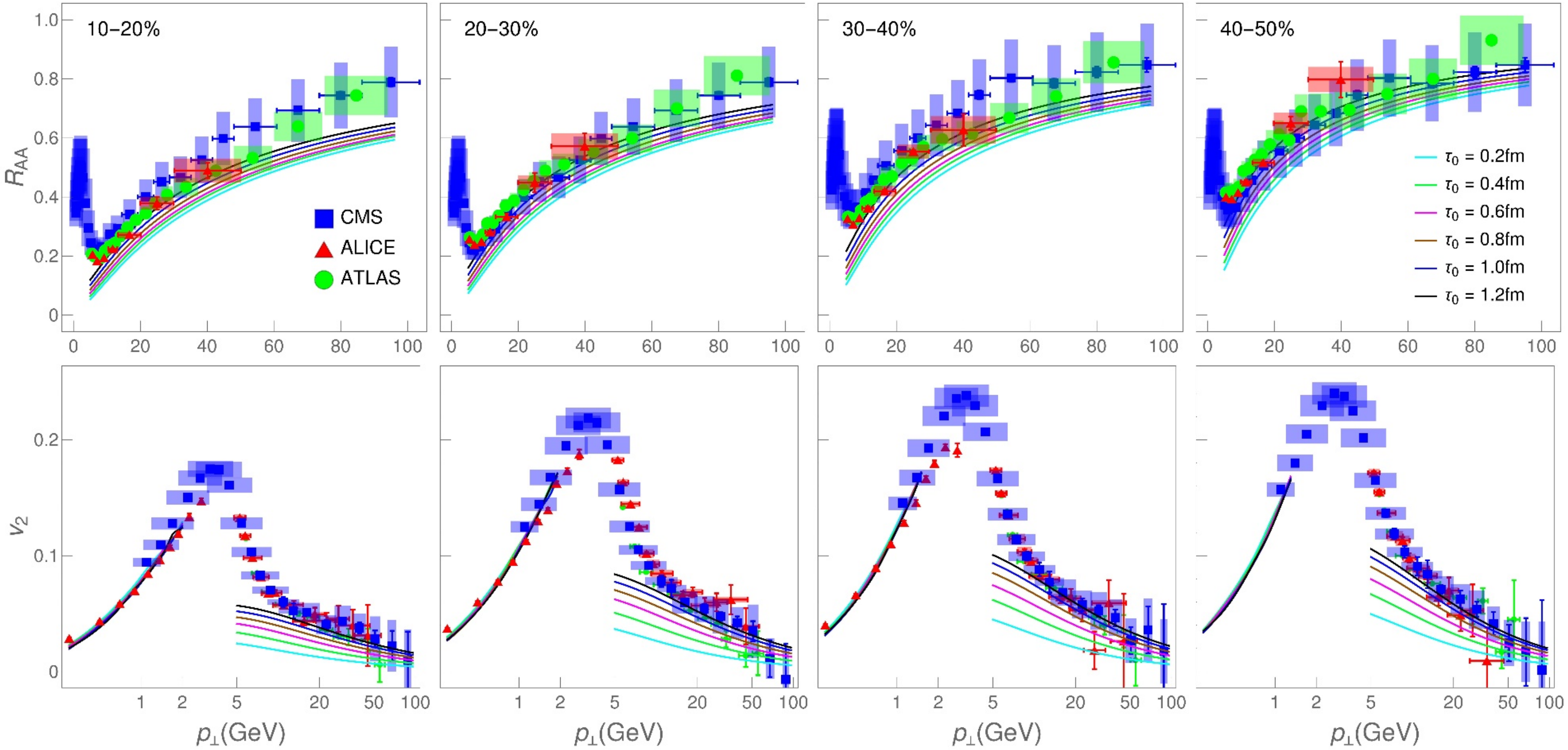

- High-p_T predictions can be clearly resolved against experimental data
  - Robustly prefer latter τ_0 for both R_{AA} and v_2.
- Larger sensitivity of v_2 predictions. Asymptotically approach the high-p_T tail of the experimental data, as τ_0 is increased.

What about more sophisticated hydro initializations?

Include more sophisticated initializations, such as EKRT, IP-Glasma, free streaming.

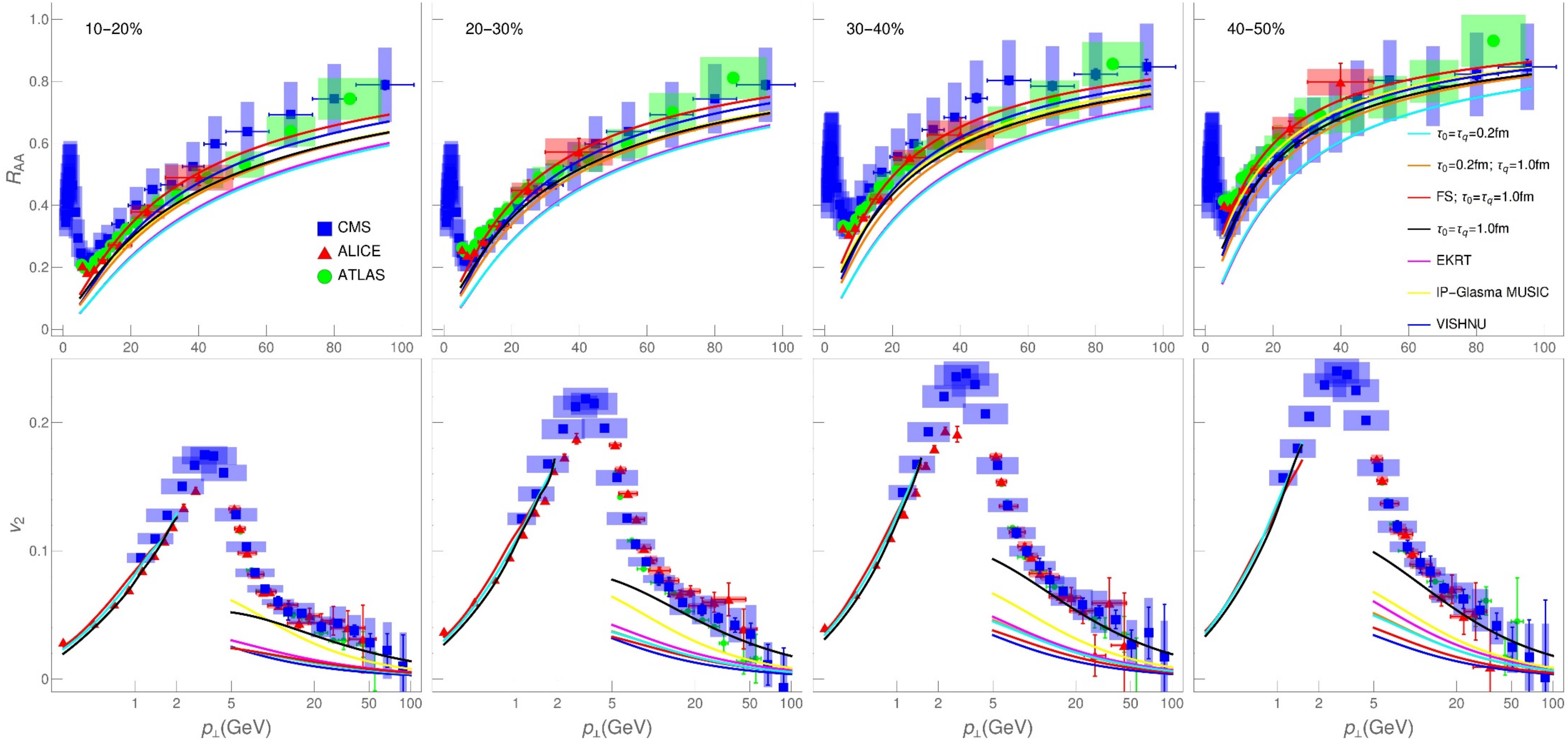

High-p_T R_{AA} and v_2 are sensitive to different initializations and early expansion dynamics, and prefer delayed onset of energy loss and transverse expansion!

S. Stojku., J. Auvinen, M. Djordjevic, P. Huovinen and MD, PRC 105, L021901

DREENA-C: Numerical framework

- Heavy flavor production

Z.B. Kang, I. Vitev, H. Xing, PLB 718, 482; R. Sharma, I. Vitev, and B. W. Zhang, PRC 80, 054902

- Dynamical energy loss in a finite size QCD medium

M. Djordjevic and M. Djordjevic, PLB 734, 286

- Multi-gluon fluctuations

M. Gyulassy, P. Levai, I. Vitev, PLB 538, 282

S. Wicks, W. Horowitz, M. Djordjevic, M. Gyulassy, NPA 784, 426

- Path-length fluctuations

A. Dainese, EPJ C33, 495; S. Wicks, W. Horowitz, M. Djordjevic and M. Gyulassy, NPA 784, 426; D. Zigic, I. Salom, J. Auvinen, M. Djordjevic and M. Djordjevic, JPG 46, 085101

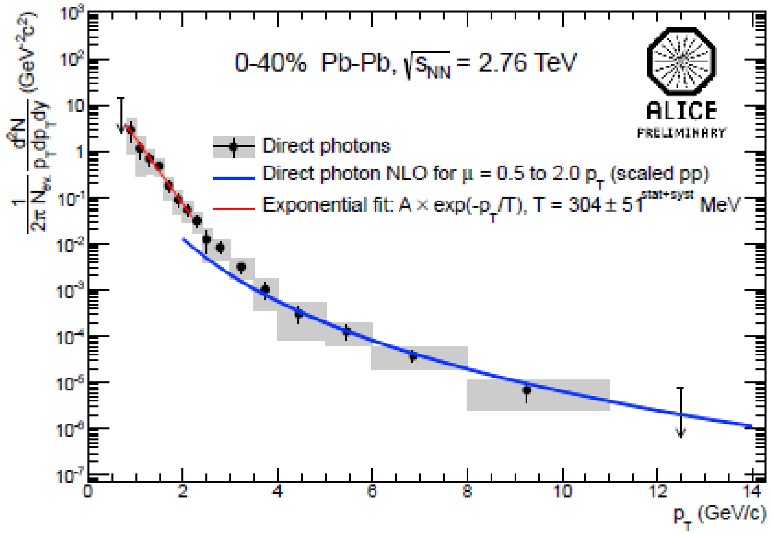

ALICE: NPA 904-905 573c

(T_{eff}) of 304 MeV for 0-40% centrality   2.76 TeV Pb+Pb

$$T^3 \sim \frac{\frac{dN_g}{dy}}{V} \rightarrow T = c\left(\frac{\frac{dN_g}{dy}}{N_{part}}\right)^{1/3}$$

For each centrality region.

$$V \sim N_{part} \qquad \frac{\frac{dN_g}{dy}}{N_{part}} \sim \frac{\frac{dN_{ch}}{dy}}{N_{part}/2}$$

measured

M. Gyulassy, P. Levai and I. Vitev, NPB 594 371
M. Djordjevic, M. Djordjevic and B. Blagojevic, PLB 737, 298

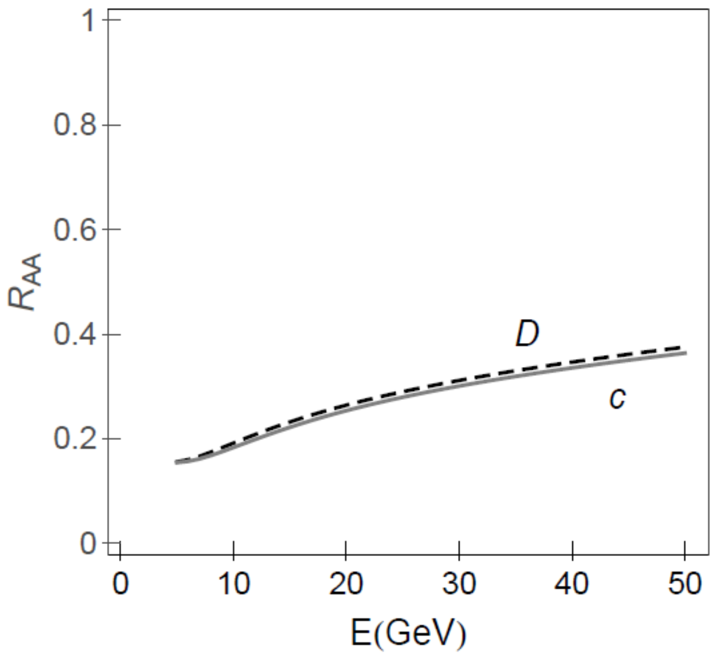

$$\frac{E_f d^3\sigma_f}{dp_f^3} = \frac{E_i d^3\sigma_i(Q)}{dp_i^3} \otimes P(E_i \rightarrow E_f)$$

PRL 112, no.4, 042302 (2014)

D and B mesons (non-prompt J/Ψ….) present genuine charm and bottom probe's suppression.

M. Djordjevic, M. Gyulassy, R. Vogt and S. Wicks, Phys. Lett. B 632, 81-86 (2006)
M. Djordjevic, Phys. Rev. Lett. 112, no.4, 042302 (2014)
M. Djordjevic, Phys. Lett. B 763, 439-444 (2016)

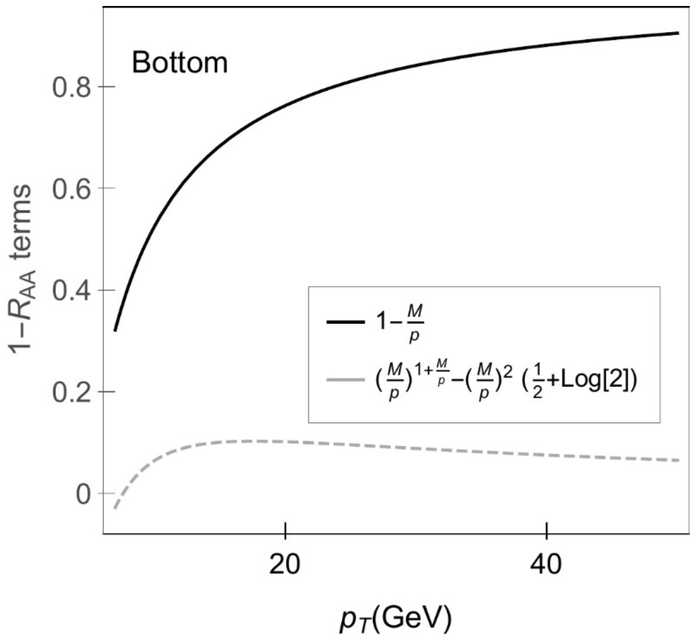
Bottom
1−R_AA terms
0.8
0.6
0.4
0.2
0
20
40
p_T(GeV)
1−M/p
(M/p)^(1+M/p)−(M/p)^2 (1/2+Log[2])

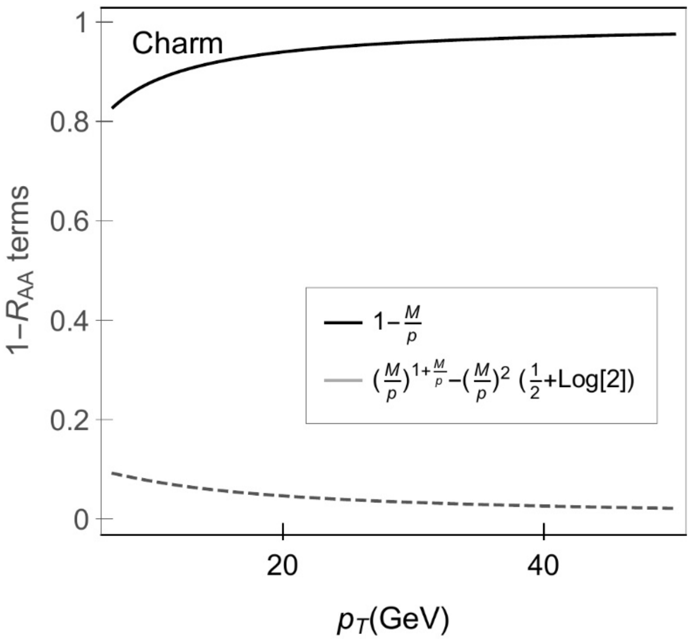
Charm
1−R_AA terms
1
0.8
0.6
0.4
0.2
0
20
40
p_T(GeV)
1−M/p
(M/p)^(1+M/p)−(M/p)^2 (1/2+Log[2])

DREENA-A Numerical framework

$$\frac{E_f d^3\sigma_q(H_Q)}{dp_f^3} = \frac{E_i d^3\sigma(Q)}{dp_i^3} \otimes P(E_i \to E_f) \otimes D(Q \to H_Q)$$

- Light and heavy flavor production

Z.B. Kang, I. Vitev, H. Xing, PLB 718, 482; R. Sharma, I. Vitev, and B. W. Zhang, PRC 80, 054902

- Dynamical energy loss in a finite size QCD medium

M. Djordjevic and M. Djordjevic, PLB 734, 286

- Multi-gluon fluctuations

M. Gyulassy, P. Levai, I. Vitev, PLB 538, 282; M. Djordjevic and M. Djordjevic, PLB 734, 286

S. Wicks, W. Horowitz, M. Djordjevic, M. Gyulassy, NPA 784, 426; G. D. Moore, D. Teaney, PRC 71, 064904

- Path-length fluctuations

Dainese, EPJ C33, 495; S. Wicks, W. Horowitz, M. Djordjevic and M. Gyulassy, NPA 784, 426; D. Zigic, I. Salom, J. Auvinen, M. Djordjevic and M. Djordjevic, JPG 46, 085101

- Fragmentation functions

DSS: D. de Florian, R. Sassot and M. Stratmann, PRD 75, 114010

BCFY: E. Braaten, K.-M. Cheung, S. Fleming and T. C. Yuan, PRD 51, 4819

KLP: V. G. Kartvelishvili, A.K. Likhoded, V.A. Petrov, PLB 78, 615

$$T_{profile}(\mathrm{x}_0 + \tau\cos\phi, \mathrm{y}_0 + \tau\sin\phi, \tau)$$

$$\frac{d^2 N_{\rm rad}}{dx d\tau} = \int \frac{d^2k}{\pi}\frac{d^2q}{\pi}\frac{2\,C_R C_2(G)\,T}{x}\frac{\mu_E(T)^2 - \mu_M(T)^2}{(\boldsymbol{q}^2 + \mu_M(T)^2)(\boldsymbol{q}^2 + \mu_E(T)^2)}\frac{\alpha_S(ET)\,\alpha_S(\frac{\boldsymbol{k}^2+\chi(T)}{x})}{\pi}$$
$$\times \frac{(\boldsymbol{k}+\boldsymbol{q})}{(\boldsymbol{k}+\boldsymbol{q})^2 + \chi(T)}\left(1 - \cos\left(\frac{(\boldsymbol{k}+\boldsymbol{q})^2 + \chi(T)}{xE^+}\tau\right)\right)\left(\frac{(\boldsymbol{k}+\boldsymbol{q})}{(\boldsymbol{k}+\boldsymbol{q})^2 + \chi(T)} - \frac{\boldsymbol{k}}{\boldsymbol{k}^2 + \chi(T)}\right)$$

$$\chi(T) \equiv M^2 x^2 + m_g(T)^2$$

$$\frac{dE_{col}}{d\tau} = \frac{2C_R}{\pi\, v^2}\alpha_S(ET)\,\alpha_S(\mu_E^2(T)) \times$$
$$\int_0^\infty n_{eq}(|\vec{\mathbf{k}}|, T)d|\vec{\mathbf{k}}| \left(\int_0^{|\vec{\mathbf{k}}|/(1+v)} d|\vec{\mathbf{q}}| \int_{-v|\vec{\mathbf{q}}|}^{v|\vec{\mathbf{q}}|} \omega d\omega + \int_{|\vec{\mathbf{k}}|/(1+v)}^{|\vec{\mathbf{q}}|_{max}} d|\vec{\mathbf{q}}| \int_{|\vec{\mathbf{q}}|-2|\vec{\mathbf{k}}|}^{v|\vec{\mathbf{q}}|} \omega d\omega\right) \times$$
$$\left(|\Delta_L(q,T)|^2 \frac{(2|\vec{\mathbf{k}}| + \omega)^2 - |\vec{\mathbf{q}}|^2}{2} + |\Delta_T(q,T)|^2 \frac{(|\vec{\mathbf{q}}|^2 - \omega^2)((2|\vec{\mathbf{k}}| + \omega)^2 + |\vec{\mathbf{q}}|^2)}{4|\vec{\mathbf{q}}|^4}(v^2|\vec{\mathbf{q}}|^2 - \omega^2)\right)$$

$$n_{eq}(|\vec{\mathbf{k}}|, T) = \frac{N}{e^{|\vec{\mathbf{k}}|/T}-1} + \frac{N_f}{e^{|\vec{\mathbf{k}}|/T}+1}$$

$$\frac{\mu_E(T)^2}{\Lambda_{QCD}^2}\ln\left(\frac{\mu_E(T)^2}{\Lambda_{QCD}^2}\right) = \frac{1 + N_f/6}{11 - 2/3\,N_f}\left(\frac{4\pi T}{\Lambda_{QCD}}\right)^2$$

$$\alpha_S(Q^2) = \frac{4\pi}{(11 - 2/3N_f)\ln(Q^2/\Lambda_{QCD}^2)}$$

Averaged evolution models

- Optical Glauber:
  - Optical Glauber initialization (τ_0=1 fm, no initial transverse flow)
  - 3+1D viscous fluid code (E. Molnar, H. Holopainen, P. Huovinen and H. Niemi, PRC 90, 044904), η/s=0.12, no bulk viscosity (for RHIC η/s=0.16)
  - EoS parametrisation s95p-PCE-v1 (P. Huovinen and P. Petreczky, NPA 837, 26-53)
- EKRT:
  - EKRT initialization (K. J. Eskola, K. Kajantie, P. V. Ruuskanen and K. Tuominen, NPB 570, 379; PRC 87, 044904; PLB 731, 126) τ_0=0.2 fm
  - 3+1D viscous fluid code with boost-invariant expansion (E. Molnar, H. Holopainen, P. Huovinen and H. Niemi, PRC 90, 044904)
  - Bayesian analysis η/s(T) (min 0.18), no bulk viscosity
  - EoS parametrization s83s$_{18}$ (J. Auvinen, K. J. Eskola, P. Huovinen, H. Niemi, R. Paatelainen and P. Petreczky, PRC 102, 044911)
- T$_R$ENTo:
  - T$_R$ENTo initialization (J. S. Moreland, J. E. Bernhard and S. A. Bass, PRC 92, 011901), with free streaming until τ_0=1.16 fm
  - VISH2+1 code (H. Song and U. W. Heinz, PRC 77, 064901; arXiv:1804.06469; NP 15, no.11, 1113-1117)
  - Bayesian analysis η/s(T) (min 0.081), ζ/s(T) (max 0.052)
  - EoS lattice (A. Bazavov et al. [HotQCD], PRD 90, 094503)

Event-by-event evolution models

- MC Glauber:
  - Monte-Carlo Glauber initialization (τ_0=1 fm, no initial transverse flow)
  - 3+1D viscous fluid code (E. Molnar, H. Holopainen, P. Huovinen and H. Niemi, PRC 90, 044904), η/s=0.03, no bulk viscosity
  - EoS parametrisation s95p-PCE-v1 (P. Huovinen and P. Petreczky, NPA 837, 26-53)
- T_RENTo:
  - T_RENTo initialization, with free streaming until τ_0=1.16 fm
  - VISH2+1 code (H. Song and U. W. Heinz, PRC 77, 064901; arXiv:1804.06469; NP 15, no.11, 1113-1117)
  - Bayesian analysis η/s(T) (min 0.081), ζ/s(T) (max 0.052)
  - EoS lattice (A. Bazavov et al. [HotQCD], PRD 90, 094503)
- IP-Glasma:
  - IP-Glasma (B. Schenke, P. Tribedy and R. Venugopalan, PRL 108, 252301; PRC 86, 034908; B. Schenke, C. Shen and P. Tribedy, PRC 102, 044905) τ_{switch}=0.4
  - MUSIC code with boost-invariant expansion (B. Schenke, S. Jeon and C. Gale, PRC 82, 014903; PRL 106, 042301; PRC 85, 024901), η/s=0.12, ζ/s(T) (max 0.13)
  - EoS HotQCD lattice (J. S. Moreland and R. A. Soltz, PRC 93, 044913)